

File ID uvapub:30108
Filename 135699y.pdf
Version unknown

SOURCE (OR PART OF THE FOLLOWING SOURCE):

Type article
Title Unoccupied electronic structure of Sr₂CuO₂Cl₂ and Ba₂Cu₃O₄Cl₂:
 experiment and theory
Author(s) S. Haffner, R. Neudert, M. Kielwein, M. Knupfer, M.S. Golden, G. Krabbes,
 J. Fink, H. Rosner, R. Hayn
Faculty UvA: Universiteitsbibliotheek
Year 1998

FULL BIBLIOGRAPHIC DETAILS:

<http://hdl.handle.net/11245/1.426775>

Copyright

It is not permitted to download or to forward/distribute the text or part of it without the consent of the author(s) and/or copyright holder(s), other than for strictly personal, individual use, unless the work is under an open content licence (like Creative Commons).

Unoccupied electronic structure of $\text{Sr}_2\text{CuO}_2\text{Cl}_2$ and $\text{Ba}_2\text{Cu}_3\text{O}_4\text{Cl}_2$: Experiment and theory

S. Haffner, R. Neudert, M. Kielwein, M. Knupfer, M. S. Golden, K. Ruck,
G. Krabbes, and J. Fink

Institut für Festkörper- und Werkstofforschung Dresden, P.O. Box 270016, D-01171 Dresden, Germany

H. Rosner and R. Hayn

Max Planck Arbeitsgruppe "Elektronensysteme," Technische Universität Dresden, D-01062 Dresden, Germany

H. Eisaki and S. Uchida

Department of Superconductivity, University of Tokyo, Bunkyo-ku, Tokyo 113, Japan

Z. Hu, M. Domke, and G. Kaindl

Institut für Experimentalphysik, Freie Universität Berlin, Arnimallee 14, D-14195 Berlin, Germany

(Received 22 August 1997)

The unoccupied electronic structure of the layered cuprates $\text{Sr}_2\text{CuO}_2\text{Cl}_2$ and $\text{Ba}_2\text{Cu}_3\text{O}_4\text{Cl}_2$ has been studied using polarization-dependent x-ray absorption spectroscopy at the O $1s$ and Cu $2p_{3/2}$ edges and band-structure calculations within the local-density approximation. In contrast to almost all high-temperature superconductors, there are no oxygen atoms outside the Cu-O planes in these oxychlorides. Our results represent therefore direct experimental information regarding the oxygen-derived unoccupied electronic structure of undoped Cu-O planes in square-planar coordination. The O $1s$ and Cu $2p_{3/2}$ x-ray absorption spectra of $\text{Sr}_2\text{CuO}_2\text{Cl}_2$ and $\text{Ba}_2\text{Cu}_3\text{O}_4\text{Cl}_2$ are quite similar with an essentially two-dimensional upper Hubbard band and extra oxygen and copper related absorption fine structure at higher energies. From its polarization dependence and a comparison to the results of the band-structure calculations, it is concluded that this extra fine structure is related to transitions into O $2p$ and Cu $3d_{3z^2-r^2}$ orbitals which have become partly unoccupied due to hybridization with Sr $4d$ /Ba $5d$ /Cu $4p_z$ and Cu $4s$ orbitals, respectively. Differences between these two compounds are the larger width of the upper Hubbard band and the higher relative Cu $3d_{3z^2-r^2}$ hole occupation above the upper Hubbard band in $\text{Ba}_2\text{Cu}_3\text{O}_4\text{Cl}_2$. These differences can be related to the extra Cu_B atoms in the Cu_3O_4 planes of $\text{Ba}_2\text{Cu}_3\text{O}_4\text{Cl}_2$ with respect to the CuO_2 planes of $\text{Sr}_2\text{CuO}_2\text{Cl}_2$. [S0163-1829(98)03706-0]

I. INTRODUCTION

The magnetic and electronic properties of layered cuprates (e.g., La_2CuO_4) have received much attention in recent years, because they are nearly ideal quantum antiferromagnets when undoped and (some of them) become high-temperature superconductors when doped. Crucial for their understanding is the knowledge of the energetically low-lying electronic structure of the CuO_2 planes [Fig. 1(a)], which are a structural element common to almost all of these materials. Electron energy-loss (EELS) and x-ray absorption spectroscopy (XAS) of layered cuprates have shown that the first electron-addition states of such cuprates, which are related to the upper Hubbard band (UHB), are dominated by Cu $3d_{x^2-y^2}$ and O $2p_{x,y}$ orbitals with only a small admixture of out-of-plane Cu $3d_{3z^2-r^2}$ and O $2p_z$ orbitals;¹ thus these materials represent nearly ideal two-dimensional quantum systems. The higher-lying O $2p$ -derived unoccupied electronic structure of the CuO_2 planes of most of the high-temperature superconductors is not directly accessible by XAS or EELS, because the O $2p$ -derived spectral weight in this energy range may be at least partially due to oxygen atoms located outside the CuO_2 planes (e.g., in the block layers). This problem does not exist in the copper oxyhalides $A_2\text{CuO}_2X_2$ and $A_2\text{Cu}_3\text{O}_4X_2$ (A : Ba, Sr; X : halide): they are layered cuprate compounds composed of Cu-O planes with

no oxygen atoms located outside the Cu-O planes.

A representative of the $A_2\text{CuO}_2X_2$ compounds is the copper oxychloride $\text{Sr}_2\text{CuO}_2\text{Cl}_2$,² which is a tetragonal antiferromagnetic insulator (Néel temperature 250 K),³ isostructural to the high-temperature phase of La_2CuO_4 , but which has apical chlorine ions instead of apical oxygen ions. The Cu-Cl_{apex} distance in $\text{Sr}_2\text{CuO}_2\text{Cl}_2$ (2.86 Å) (Ref. 2) is significantly larger than the Cu-O_{apex} distance in La_2CuO_4 (2.42 Å) (Ref. 4) making it an interesting candidate for a model system describing the physics of an undoped CuO_2 plane because of the reduced influence of the out-of-plane ions on the CuO_2 planes. Magnetization and neutron scattering experiments^{3,5} have indeed shown that $\text{Sr}_2\text{CuO}_2\text{Cl}_2$ can be regarded as the best experimental realization of the $S=1/2$ two-dimensional square lattice Heisenberg antiferromagnet known up to now. Although until now it was not possible to dope $\text{Sr}_2\text{CuO}_2\text{Cl}_2$ chemically in order to achieve a metallic or even superconducting state⁶ (thus, strictly it is not a parent compound of a high-temperature superconductor), it is also an interesting model system for the study of aspects of high-temperature superconductivity, because in a photoemission experiment $\text{Sr}_2\text{CuO}_2\text{Cl}_2$ is hole doped by the photoionization process itself, such that the electronic structure of a CuO_2 plane in the low-doping limit can be studied. The energy-momentum relation of the hole thus created can be measured, which in the case of the lowest electron

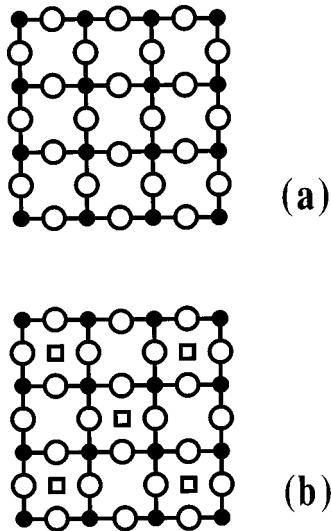


FIG. 1. Sketch of the Cu-O plane geometries. (a) CuO_2 plane of $\text{Sr}_2\text{CuO}_2\text{Cl}_2$ (● Cu atoms, ○ O atoms). (b) Cu_3O_4 plane of $\text{Ba}_2\text{Cu}_3\text{O}_4\text{Cl}_2$ (● Cu_A atoms, □ Cu_B atoms, ○ O atoms).

removal states corresponds to a determination of the dispersion of a Zhang-Rice singlet⁷ in an antiferromagnetic background (if the size of the “magnetic polaron” is much smaller than the antiferromagnetic correlation length⁸).⁹ Experiments of this kind have not been possible up to now with the insulating parent compounds of the high-temperature superconductors, because they do not satisfy the high demands of photoemission spectroscopy on surface quality (in contrast to $\text{Sr}_2\text{CuO}_2\text{Cl}_2$).

Representatives of the $\text{A}_2\text{Cu}_3\text{O}_4\text{X}_2$ compounds are the tetragonal insulators $\text{Ba}_2\text{Cu}_3\text{O}_4\text{Cl}_2$ and $\text{Sr}_2\text{Cu}_3\text{O}_4\text{Cl}_2$.¹⁰ They are composed of Cu_3O_4 planes [Fig. 1(b)] as fundamental building blocks, which in contrast to CuO_2 planes have two different copper sites: two-thirds of the Cu atoms (Cu_A) occupy the Cu sites of the familiar CuO_2 plane, while one-third of the Cu atoms (Cu_B) reside in the center of every second CuO_4 square. The distances from the Cu_A and Cu_B atoms to their apical ions ($\text{Cu}_A\text{-Cl}_{\text{apex}}$: 3.46 Å, $\text{Cu}_B\text{-Ba}_{\text{apex}}$: 4.99 Å) are even larger than the $\text{Cu-Cl}_{\text{apex}}$ distance in $\text{Sr}_2\text{CuO}_2\text{Cl}_2$. These compounds exhibit interesting magnetic properties which are directly related to the existence of two different Cu sublattices. Two antiferromagnetic transition temperatures have been measured: the first transition occurring at 320 and 380 K for $\text{Ba}_2\text{Cu}_3\text{O}_4\text{Cl}_2$ and $\text{Sr}_2\text{Cu}_3\text{O}_4\text{Cl}_2$,^{11–13} respectively. These temperatures are comparable to the Néel temperatures of other cuprates and are ascribed to antiferromagnetic order in the Cu_A sublattice. The second transition is at 30 K for $\text{Ba}_2\text{Cu}_3\text{O}_4\text{Cl}_2$ and 40 K for $\text{Sr}_2\text{Cu}_3\text{O}_4\text{Cl}_2$,^{11–13} and marks the onset of antiferromagnetic order in the Cu_B subsystem. In the temperature range between the two antiferromagnetic transitions a weak in-plane ferromagnetic component has also been found which has been explained by a pseudodipolar coupling between the Cu subsystems in the case of $\text{Sr}_2\text{Cu}_3\text{O}_4\text{Cl}_2$.¹³ According to magnetization and neutron scattering experiments,¹³ both the Cu_A and Cu_B subsystems of $\text{Sr}_2\text{Cu}_3\text{O}_4\text{Cl}_2$ represent further examples of $S=1/2$ two-dimensional quantum antiferromagnets. The Cu_B subsystems of $\text{Sr}_2\text{Cu}_3\text{O}_4\text{Cl}_2$ and $\text{Ba}_2\text{Cu}_3\text{O}_4\text{Cl}_2$ are especially interesting because of their weak exchange interaction ($J\sim 10$ and 17

meV, respectively),^{13,14} which is an order of magnitude smaller than the exchange interaction normally encountered in systems of corner-sharing CuO_4 plaquettes ($J\sim 125$ meV).¹⁵ These compounds also offer the exciting possibility of the determination of the dispersion of a Zhang-Rice singlet moving in an antiferromagnetic ($\text{Cu}_A\text{-O}$ subsystem) and a paramagnetic ($\text{Cu}_B\text{-O}$ subsystem) background in a single room-temperature photoemission experiment. This has been carried out for $\text{Ba}_2\text{Cu}_3\text{O}_4\text{Cl}_2$ (Ref. 8) and corresponds to the simultaneous study of the low- and high-doping limit of a CuO_2 plane as far as the magnetic background is concerned. In this paper, we examine the unoccupied O $2p$ and Cu $3d$ -derived electronic structure of $\text{Sr}_2\text{CuO}_2\text{Cl}_2$ and $\text{Ba}_2\text{Cu}_3\text{O}_4\text{Cl}_2$ using polarization-dependent O $1s$ and Cu $2p_{3/2}$ XAS at room temperature and band-structure calculations in the local-density approximation (LDA).

II. EXPERIMENTAL AND THEORETICAL METHODS

$\text{Sr}_2\text{CuO}_2\text{Cl}_2$ single crystals were grown by the traveling-solvent floating-zone technique and had dimensions up to $10\times 5\times 1.5$ mm. The $\text{Ba}_2\text{Cu}_3\text{O}_4\text{Cl}_2$ single crystals were grown from the melt, their typical dimensions being $2.5\times 2\times 0.7$ mm.

The XAS measurements were performed with linearly polarized synchrotron radiation obtained from the SX 700/II monochromator¹⁶ operated by the *Freie Universität Berlin* at the *Berliner Elektronenspeicherring für Synchrotronstrahlung* (BESSY). Total electron yield (TEY) as well as fluorescence yield (FY) have been applied to monitor the absorption at the O $1s$ and Cu $2p$ edges, the energy resolution being set to 280 and 660 meV for the O $1s$ and Cu $2p$ absorption thresholds, respectively. Cleaved and as-grown surfaces were used for the FY measurements of $\text{Sr}_2\text{CuO}_2\text{Cl}_2$ and $\text{Ba}_2\text{Cu}_3\text{O}_4\text{Cl}_2$, respectively. For the surface-sensitive TEY measurements only cleaved surfaces were used. The single crystals were cleaved *in situ* at a base pressure of 2×10^{-10} mbar by means of a cantilever attached to the top of the sample, resulting in a cleavage plane which is parallel to the $\text{CuO}_2/\text{Cu}_3\text{O}_4$ planes. All measurements were performed at room temperature.

In order to study the polarization dependence of the XAS signal, different angles of incidence of the x-ray beam with respect to the $\text{CuO}_2/\text{Cu}_3\text{O}_4$ planes were used. In the geometry of normal incidence, the electric-field vector of the incoming radiation lies in the $\text{CuO}_2/\text{Cu}_3\text{O}_4$ planes (“in-plane geometry”). In the case of $\text{Sr}_2\text{CuO}_2\text{Cl}_2$, spectra for the electric-field vector perpendicular to the CuO_2 planes (“out-of-plane geometry”) were extrapolated from measurements at grazing incidence at three different incidence angles (50° , 55° , 65°) with respect to the CuO_2 planes. In the case of $\text{Ba}_2\text{Cu}_3\text{O}_4\text{Cl}_2$, FY measurements in out-of-plane geometry were performed at a side face of the crystals at normal incidence. The data have been corrected for the time dependence of the incident photon flux by means of the simultaneously measured ring current of the synchrotron. The energy dependence of the incident photon flux was taken into account via division by an XAS spectrum of a clean gold foil recorded in the same energy range. A linear background has been subtracted. Additionally, the spectra were normalized to calculated atomic O $1s$ and Cu $2p$ photoionization cross

sections¹⁷ ~ 70 eV above the absorption threshold. This far above the threshold, the final states are practically free-electron-like and thus isotropic. Self-absorption effects were taken into account according to a procedure described elsewhere,¹⁸ and the energy calibration was checked by comparison of CuO Cu $2p_{3/2}$ TEY data measured during these experiments with corresponding data in the literature.¹⁹

The density of states (DOS) and the partial DOS for both compounds were calculated in the LDA using the linear combination of atomic orbitals method. Due to the relatively open structures, four and eight empty spheres per unit cell have been introduced for Sr₂CuO₂Cl₂ and Ba₂Cu₃O₄Cl₂, respectively. The calculations are scalar relativistic and a minimal basis was chosen consisting of Cu($4s,4p,3d$), O($2s,2p$), Ba($6s,6p,5d$), Sr($5s,5p,4d$), and Cl($3s,3p$). The lower-lying states were treated as core states. To optimize the local basis a contraction potential has been used at each site.²⁰ The Coulomb part of the potential was constructed as a sum of overlapping spherical contributions and the exchange and correlation part was treated in the atomic-sphere approximation. The orbital-projected partial DOS and the corresponding hole occupation numbers are calculated as net quantities. In order to facilitate comparison with experiment, the calculated partial DOS were broadened by convolution with a Lorentzian and a Gaussian to account for lifetime effects and the experimental energy resolution, respectively. A linear energy dependence of the lifetime was assumed.

III. RESULTS AND DISCUSSION

In XAS experiments, core electrons are excited into unoccupied states by absorption of photons. This leaves the solid in an excited state which decays via emission of fluorescence photons (FY) or electrons (TEY), whose intensity is measured as a function of the energy of the incoming photons. The mean escape depth of the electrons is of the order of 10 Å. Therefore TEY is a surface-sensitive method in contrast to FY which probes bulk properties (mean escape depth of soft-x-ray photons: 10 000 Å). As core electrons are localized, the local unoccupied electronic structure is probed (XAS is site-selective). The transitions of the core electrons into the unoccupied states are governed by dipole selection rules. Therefore, in recording an O $1s$ (Cu $2p$) x-ray absorption spectrum one measures mainly the O $2p$ (Cu $3d$) orbital contributions to the matrix-element weighted unoccupied density of states,²¹ under the supposition that the influence of the core hole in the final state on the x-ray absorption spectrum can be neglected. It is generally accepted that O $1s$ x-ray absorption spectra of cuprates are not distorted by the interaction with the core hole. This is not true for Cu $2p$ x-ray absorption spectra, where spectral weight is shifted from higher energies to the threshold due to the interaction of the localized excited d -electron with the core hole to give the so-called “white-line.” The spectral weight thus no longer reflects the detailed shape of the unoccupied Cu $3d$ derived electronic structure, but its intensity is nevertheless related to the number of holes in the Cu $3d$ shell.¹ The usage of polarized radiation and a single-crystalline sample imposes further restrictions on the symmetry of the unoccupied states which are observable in an absorption spectrum: if the electric-field vector is in the CuO₂/Cu₃O₄ plane, there are

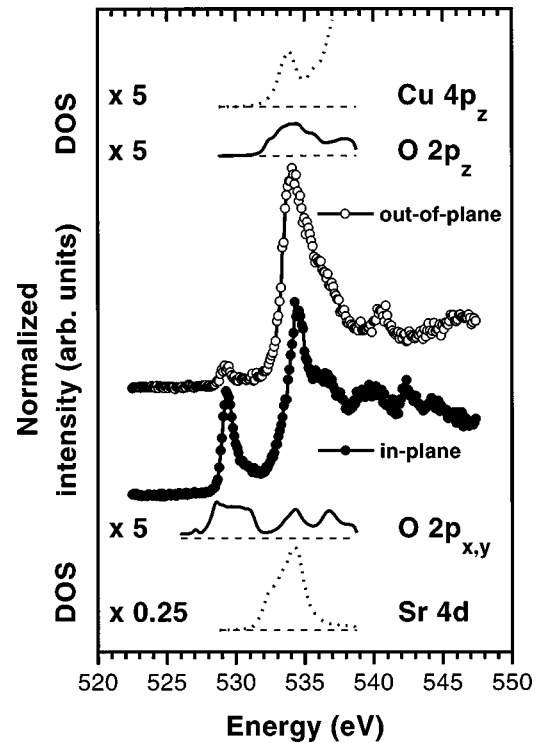


FIG. 2. O $1s$ x-ray absorption spectra of Sr₂CuO₂Cl₂. ●- : electric-field vector in the CuO₂ plane; ○- : electric-field vector perpendicular to the CuO₂ plane. The solid lines show calculated O $2p_x$ and O $2p_z$ partial DOS as indicated in the figure. In order to illustrate hybridization effects the calculated Sr $4d$ and Cu $4p_z$ partial DOS are included as dotted lines. They should not be directly compared with the experimental data which are a measure of the unoccupied O $2p$ partial DOS. The DOS curves are broadened for lifetime effects and resolution and are shifted in energy to facilitate comparison with experiment (for details see text).

only contributions from unoccupied in-plane p orbitals (p_x, p_y) and unoccupied in- and out-of-plane d orbitals ($d_{x^2-y^2}, d_{3z^2-r^2}$) to the O $1s$ and Cu $2p$ x-ray absorption spectra, respectively, while for the electric-field perpendicular to the CuO₂/Cu₃O₄ planes only out-of-plane orbitals ($p_z, d_{3z^2-r^2}$) are probed.¹

Figures 2 and 3 present polarization-dependent O $1s$ x-ray absorption spectra (FY) of Sr₂CuO₂Cl₂ and Ba₂Cu₃O₄Cl₂ for in- and out-of-plane geometry. In addition, calculated Sr $4d$ /Ba $5d$, O $2p_{x,y}$, O $2p_z$, and Cu $4p_z$ partial DOS are shown. All of the calculated partial DOS are shifted in energy by the amount necessary to get best agreement between the calculated O $2p$ partial DOS and experiment. The overall shape of the experimental O $1s$ x-ray absorption spectra is essentially the same for both compounds: they consist of a broad absorption feature at ~ 534 and ~ 533 eV and a prepeak at 529.4 and 529.8 eV for Sr₂CuO₂Cl₂ and Ba₂Cu₃O₄Cl₂, respectively. Both compounds show anisotropy in intensity between absorption spectra taken in in- and out-of-plane geometry; this is especially distinct in the case of the prepeaks, which are considerably stronger when the electric-field vector is in-plane.

The prepeaks are associated with the O $2p$ contributions to the upper Hubbard band,¹ and the anisotropy between in-plane and out-of-plane geometry reveals that these are predominantly from in-plane oxygen orbitals (O $2p_x, O 2p_y$),

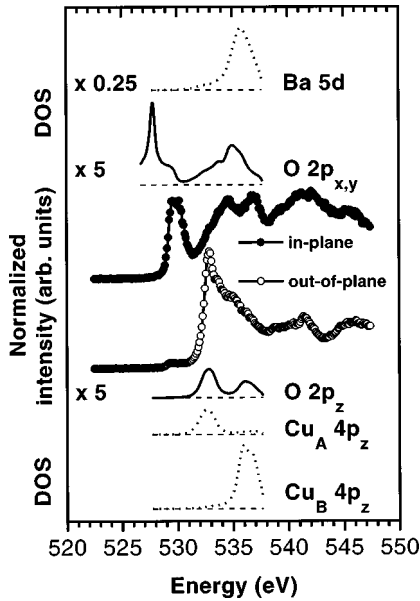


FIG. 3. O $1s$ x-ray absorption spectra of $\text{Ba}_2\text{Cu}_3\text{O}_4\text{Cl}_2$. \bullet : electric-field vector in the Cu_3O_4 plane; \circ : electric-field vector perpendicular to the Cu_3O_4 plane. The solid lines show calculated O $2p_x$ and O $2p_z$ partial DOS as indicated in the figure. In order to illustrate hybridization effects the calculated Ba $5d$ and $\text{Cu}_{A,B}$ $4p_z$ partial DOS are included as dotted lines. They should not be directly compared with the experimental data which are a measure of the unoccupied O $2p$ partial DOS. The DOS curves are broadened for lifetime effects and resolution and are shifted in energy to facilitate comparison with experiment (for details see text).

while out-of-plane oxygen orbitals (O $2p_z$) contribute significantly less. A comparison of the spectral weights of the prepeaks for in- and out-of-plane geometry yields values of 0.13 ($\text{Sr}_2\text{CuO}_2\text{Cl}_2$) and 0.09 ($\text{Ba}_2\text{Cu}_3\text{O}_4\text{Cl}_2$) for the ratio of the O $2p_z$ to the total O $2p$ orbital contributions to the upper Hubbard band, these values are comparable to that measured in the cuprate high-temperature superconductors.¹ One has to keep in mind that the values given for the relative contributions of the out-of-plane orbitals are upper limits because of the possibility of a small misorientation of the crystals and the finite degree of linear polarization of the radiation (97%), so the true values may even be smaller. In Table I the calculated hole occupation numbers of the O $2p$, Cu $3d$, Cu $4s$, and Cu $4p$ orbitals are given. No O $2p_z$ orbital contribution to the UHB is found for both compounds which is in qualitative agreement with the experimental results. Two remarks concerning the result of the calculations have to be made:

(a) The calculations predict a paramagnetic and metallic behavior. This is a typical result for an LDA calculation and shows the necessity to deal with the electron correlations in a more direct way. However for the higher-lying unoccupied DOS considered here the correlations are not so important due to the small Cu $3d$ character of the higher lying bands. The main feature which will occur if we introduce the correlations explicitly is the splitting of the bands crossing the Fermi level into a lower and an upper Hubbard band (UHB). The hole occupation number for a certain orbital contribution to the UHB is therefore calculated by summing up the corresponding partial DOS from the Fermi level to the upper band edge of the Cu $3d_{x^2-y^2}$ -O $2p_{x,y}$ band.

TABLE I. Calculated total number of holes in the Cu $3d$, Cu $4p$, Cu $4s$, and O $2p$ orbitals for $\text{Sr}_2\text{CuO}_2\text{Cl}_2$ and $\text{Ba}_2\text{Cu}_3\text{O}_4\text{Cl}_2$, and the corresponding hole numbers for the upper Hubbard band alone.

Orbital	$\text{Sr}_2\text{CuO}_2\text{Cl}_2$		$\text{Ba}_2\text{Cu}_3\text{O}_4\text{Cl}_2$	
	UHB	Total	UHB	Total
Cu_A $3d_{x^2-y^2}$	0.65	0.69	0.48	0.52
Cu_A $3d_{3z^2-r^2}$		0.07		0.34
Cu_A $3d_{xy}$				0.02
Cu_A $3d_{xz,yz}$		0.02		0.02
Cu_B $3d_{x^2-y^2}$			0.74	0.75
Cu_B $3d_{3z^2-r^2}$				0.11
Cu_B $3d_{xy}$				
Cu_B $3d_{xz,yz}$				
Cu_A $4p_{x,y}$		1.87		1.92
Cu_A $4p_z$		1.91		1.94
Cu_B $4p_{x,y}$				1.95
Cu_B $4p_z$				1.95
Cu_A $4s$		1.58		1.61
Cu_B $4s$				1.63
O $2p_{x,y}$	0.08	0.63	0.17	0.69
O $2p_z$		0.32		0.20

(b) The calculated O $2p$ hole occupation numbers are given for symmetrized oxygen orbitals (linear combinations of two oxygen orbitals). This means that in the case of the UHB of $\text{Sr}_2\text{CuO}_2\text{Cl}_2$ the value given for the hole occupation number of the O $2p_{x,y}$ orbitals has to be multiplied by a factor of 2, because only one oxygen orbital per symmetrized orbital is hybridized with a Cu $3d_{x^2-y^2}$ orbital.²²

Returning to the XAS spectra, the prepeak of the $\text{Ba}_2\text{Cu}_3\text{O}_4\text{Cl}_2$ O $1s$ x-ray absorption spectrum is considerably broader (full width at half maximum, FWHM = 1.6 eV) than its $\text{Sr}_2\text{CuO}_2\text{Cl}_2$ counterpart (FWHM = 1.1 eV) and has gained $\sim 20\%$ in spectral weight. Its shape is consistent with the presence of two peaks associated with the UHB's of the Cu_A -O and Cu_B -O networks which are energetically slightly offset. As all oxygen sites in $\text{Ba}_2\text{Cu}_3\text{O}_4\text{Cl}_2$ are equivalent, this shift must be related to a difference in the energies of the Cu_A and the Cu_B $3d_{x^2-y^2}$ levels, a finding which has also been deduced from a tight-binding fit to an LDA band-structure calculation from which an energy difference of ~ 0.4 eV was found.¹⁴

In the O $2p$ -derived absorption fine structure above the UHB (above 532 eV), there are marked differences between $\text{Sr}_2\text{CuO}_2\text{Cl}_2$ and $\text{Ba}_2\text{Cu}_3\text{O}_4\text{Cl}_2$: in $\text{Sr}_2\text{CuO}_2\text{Cl}_2$ a rather isotropic peak is visible at ~ 534 eV, while its counterpart in $\text{Ba}_2\text{Cu}_3\text{O}_4\text{Cl}_2$ is located at ~ 533 eV and is much stronger in out-of-plane than in in-plane geometry. Above 533/534 eV the O $1s$ x-ray absorption spectra of $\text{Sr}_2\text{CuO}_2\text{Cl}_2$ and $\text{Ba}_2\text{Cu}_3\text{O}_4\text{Cl}_2$ are qualitatively similar with both having more spectral weight due to O $2p_{x,y}$ than O $2p_z$ orbitals.

The occurrence of O $2p$ -derived absorption fine structure above the UHB is not compatible with models of the low-lying unoccupied electronic structure of the Cu-O planes of layered cuprates which only take into account hybridization between the O $2p_{x,y}$ and the Cu $3d_{x^2-y^2}$ orbitals. Therefore there must be additional hybridization of O $2p$ orbitals with

orbitals other than the Cu $3d_{x^2-y^2}$. To gain information about the character of the other states hybridized with the O $2p$ orbitals, we compare the x-ray absorption spectra with the calculated partial DOS. The calculated partial DOS show that there is hybridization between the O $2p$ and all the other orbitals [Cu($4s, 4p, 3d$), Sr($5s, 5p, 4d$)/Ba($6s, 6p, 5d$), Cl($3s, 3p$)] which have been included in the calculation. In the following, the discussion will be limited to the dominant orbital contributions to the absorption fine structure above the UHB.

In the case of Ba₂Cu₃O₄Cl₂ (Fig. 3), the O $2p_{x,y}$ orbitals hybridize predominantly with the Ba $5d$ orbitals, while the O $2p_z$ orbitals hybridize strongest with the Cu_{A,B} $4p_z$ orbitals. The Cu_{A,B} $4p_{x,y}$ unoccupied partial DOS (not shown in Fig. 3) is of similar magnitude to the Cu_{A,B} $4p_z$ partial DOS (see Table I), but has negligible weight where the O $2p_{x,y}$ partial DOS has appreciable weight, therefore it is concluded that the hybridization between the Cu_{A,B} $4p_{x,y}$ and the O $2p_{x,y}$ orbitals is relatively weak. The calculations correctly display the observed polarization dependence: the peak at 533 eV, which is only visible in out-of-plane geometry corresponds to states of O $2p_z$ and Cu $4p_z$ character, while the calculated O $2p_{x,y}$ and Ba $5d$ partial DOS are negligible at this energy, being of importance at higher energies, where the in-plane O $1s$ x-ray absorption spectrum is indeed stronger than the out-of-plane spectrum. The relative intensities of the calculated Cu_{A,B} $4p_z$ partial DOS also explain why the peak at 533 eV is not broadened with respect to its Sr₂CuO₂Cl₂ counterpart due to the two different Cu sites (in contrast to the UHB): this peak corresponds to states whose O $2p_z$ /Cu_B $4p_z$ hybridization is negligible with respect to the O $2p_z$ /Cu_A $4p_z$ hybridization, so there is no influence of the possible differences in the on-site energies of the Cu_A $4p_z$ and Cu_B $4p_z$ levels. Hybridization between O $2p_z$ and Cu_B $4p_z$ orbitals becomes more important at higher energies and may give rise to the weak shoulder at 535 eV on the high-energy side of the O $2p_z$ /Cu_A $4p_z$ related peak. While the calculated partial DOS are qualitatively in good agreement with the experimental results, this is not the case for the calculated O $2p_{x,y}$ and O $2p_z$ hole occupation numbers above the UHB (Ref. 23) (Table I): a value of 0.38 is predicted for the ratio of the O $2p_z$ to the O $2p_{x,y}$ hole occupation numbers, while the ratio of the integrated²⁴ measured out-of-plane to in-plane spectral weights above the UHB is close to unity.

In the case of Sr₂CuO₂Cl₂ (Fig. 2) the situation is less clear. The Sr $4d$ partial DOS peaks at 534.3 eV as does the O $2p_x$ partial DOS, while the Cu $4p_z$ partial DOS has a peak at 533.9 eV. In the O $1s$ x-ray absorption spectrum there is a corresponding peak at 534.3 eV in the in-plane spectrum while it is slightly displaced in the out-of-plane spectrum to lower energy (~ 534 eV). It is therefore assumed that, as in the case of Ba₂Cu₃O₄Cl₂, the O $2p_z$ orbitals hybridize mainly with the Cu $4p_z$ orbitals while the O $2p_{x,y}$ orbitals hybridize strongest with the Sr $4d$ orbitals. As in the case of Ba₂Cu₃O₄Cl₂ the calculated O $2p$, Sr $4d$, and Cu $4p_z$ partial DOS correctly display the experimentally found polarization dependence. The calculated ratio of the O $2p_z$ to the O $2p_{x,y}$ hole occupation numbers (0.58) is as in the case of Ba₂Cu₃O₄Cl₂ too small [experiment (Ref. 24): ~ 1.0].

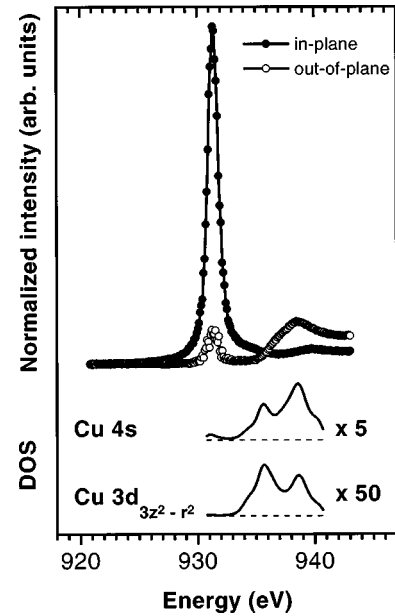


FIG. 4. Cu $2p_{3/2}$ x-ray absorption spectra of Sr₂CuO₂Cl₂. ●- : electric-field vector in the CuO₂ plane; ○- : electric-field vector perpendicular to the CuO₂ plane. The solid lines show calculated Cu $4s$ and Cu $3d_{3z^2-r^2}$ partial DOS as indicated in the figure. The DOS curves are broadened for lifetime effects and resolution and are shifted in energy to facilitate comparison with experiment (for details see text).

The differences between the O $1s$ x-ray absorption spectra above the UHB of Sr₂CuO₂Cl₂ and Ba₂Cu₃O₄Cl₂ could have their origin in the presence of the extra Cu_B atoms and the correspondingly more closed structure of the Cu₃O₄ planes in Ba₂Cu₃O₄Cl₂: because of the extra hybridization of O $2p_{x,y}$ orbitals with the Cu_B $3d_{x^2-y^2}$ orbitals, the hybridization with the Ba $5d$ orbitals is weaker than it would be without the Cu_B atoms. Therefore the spectral weight in the O $1s$ x-ray absorption spectrum, which is related to the hybridization of the alkaline-earth atoms with the O $2p_{x,y}$ orbitals, is smaller (or even absent as the peak at 534 eV) in Ba₂Cu₃O₄Cl₂ compared to Sr₂CuO₂Cl₂, while the UHB-related spectral weight is larger. The larger alkaline-earth-oxygen distance in Ba₂Cu₃O₄Cl₂ ($d_{\text{Ba-O}}$: 2.74 Å, $d_{\text{Sr-O}}$: 2.6 Å) may reinforce this effect.

Figures 4 and 5 present the polarization-dependent Cu $2p_{3/2}$ x-ray absorption spectra of Sr₂CuO₂Cl₂ (TEY) and Ba₂Cu₃O₄Cl₂ (FY) for in- and out-of-plane geometry and the calculated Cu $3d_{3z^2-r^2}$ and Cu $4s$ partial DOS. All of the calculated partial DOS are shifted in energy by the amount necessary to get the best agreement between the calculated Cu $3d_{3z^2-r^2}$ partial DOS and experiment. FY measurements are shown for Ba₂Cu₃O₄Cl₂, because it was not possible to perform TEY measurements in out-of-plane geometry on the Ba₂Cu₃O₄Cl₂ single crystals: they were too small for grazing incidence measurements at the cleavage plane of the crystals. On the other hand, there was no possibility of the preparation of a cleavage plane at 90° to the Cu₃O₄ planes where TEY measurements in an out-of-plane geometry could be accomplished by a normal-incidence measurement. For the FY mode cleaved surfaces are not necessary, we have therefore performed the Cu $2p_{3/2}$ x-ray absorption spectra in in- and out-of-plane geometry in the FY mode on as-grown surfaces

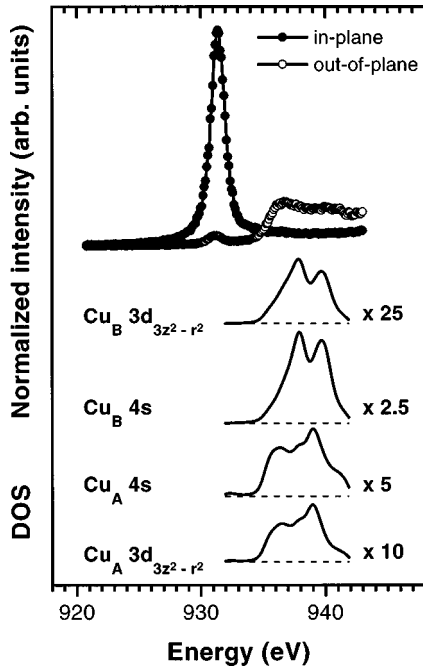


FIG. 5. Cu $2p_{3/2}$ x-ray absorption spectra of $\text{Ba}_2\text{Cu}_3\text{O}_4\text{Cl}_2$. \bullet —: electric-field vector in the Cu_3O_4 plane; \circ —: electric-field vector perpendicular to the Cu_3O_4 plane. The solid lines show calculated $\text{Cu}_{A,B}$ $4s$ and $\text{Cu}_{A,B}$ $3d_{3z^2-r^2}$ partial DOS as indicated in the figure. The DOS curves are broadened for lifetime effects and resolution and are shifted in energy to facilitate comparison with experiment (for details see text).

of the $\text{Ba}_2\text{Cu}_3\text{O}_4\text{Cl}_2$ crystals. The white line of the Cu $2p_{3/2}$ FY x-ray absorption spectrum of $\text{Ba}_2\text{Cu}_3\text{O}_4\text{Cl}_2$ is especially affected by self-absorption effects because of its high intensity. A comparison of the Cu $2p_{3/2}$ FY and TEY spectra taken in in-plane geometry shows that the FY in-plane spectra after correction for self-absorption are nevertheless equivalent to their TEY counterparts. For the Cu $2p_{3/2}$ absorption spectra recorded in out-of-plane geometry in the FY mode, there are no pronounced self-absorption effects expected because of the low intensity. We assume therefore in the following that we can rely on the relative intensities of the $\text{Ba}_2\text{Cu}_3\text{O}_4\text{Cl}_2$ Cu $2p_{3/2}$ FY spectra.

The experimental spectra show a narrow peak at 931.4 eV (the white line), which is associated with the Cu $3d$ contributions to the upper Hubbard band.¹ The spectral weights of the white lines recorded in in-plane geometry are much larger than those in out-of-plane geometry, showing that the Cu $3d$ contributions to the upper Hubbard band are also mainly from in-plane Cu $3d_{x^2-y^2}$ orbitals. A comparison of the spectral weights of the white lines recorded in in- and out-of-plane geometry yields for the ratio of the Cu $3d_{3z^2-r^2}$ to the total Cu $3d$ orbital contribution a value of 0.05 for both $\text{Sr}_2\text{CuO}_2\text{Cl}_2$ and $\text{Ba}_2\text{Cu}_3\text{O}_4\text{Cl}_2$.²⁵ The white line of $\text{Ba}_2\text{Cu}_3\text{O}_4\text{Cl}_2$ is (as in the case of the prepeak of the O $1s$ x-ray absorption spectra) significantly broader (FWHM = 1.6 eV) than that of $\text{Sr}_2\text{CuO}_2\text{Cl}_2$ (FWHM = 1.1 eV). This again is related to the presence of the extra Cu_B -O network in $\text{Ba}_2\text{Cu}_3\text{O}_4\text{Cl}_2$.

The Cu $2p_{3/2}$ x-ray absorption spectra of $\text{Sr}_2\text{CuO}_2\text{Cl}_2$ and $\text{Ba}_2\text{Cu}_3\text{O}_4\text{Cl}_2$ also show—besides the white line—a strongly

polarization-dependent absorption step at 938 and 936 eV, respectively. According to the observed polarization dependence and matrix elements, these steps must be related to transitions mainly into unoccupied Cu $3d_{3z^2-r^2}$ states. The two steps differ in their shapes and their relative intensities:

(a) there is one peak and one shoulder visible in the $\text{Sr}_2\text{CuO}_2\text{Cl}_2$ absorption step (at 938.6 and 936.7 eV, respectively), while there are two peaks in the case of $\text{Ba}_2\text{Cu}_3\text{O}_4\text{Cl}_2$ at 936.5 and around 940.7 eV.

(b) the ratio of the integrated²⁴ Cu $3d_{3z^2-r^2}$ -derived spectral weight of these absorption steps to the integrated Cu $3d_{x^2-y^2}$ -derived spectral weight of the UHB (Ref. 25) is 0.24 and 0.47 for $\text{Sr}_2\text{CuO}_2\text{Cl}_2$ and $\text{Ba}_2\text{Cu}_3\text{O}_4\text{Cl}_2$, respectively.

Absorption steps of this kind have also been seen in other cuprates.¹ From a comparison to the calculated partial DOS we conclude that (in the case of $\text{Sr}_2\text{CuO}_2\text{Cl}_2$ and $\text{Ba}_2\text{Cu}_3\text{O}_4\text{Cl}_2$ at least) they are due to Cu $3d_{3z^2-r^2}$ states which become unoccupied by hybridization with Cu $4s$ states, because the calculated Cu $3d_{3z^2-r^2}$ and Cu $4s$ partial DOS show excellent mutual agreement in shape and energetic position. Furthermore it is evident that the first peak in the absorption step of $\text{Ba}_2\text{Cu}_3\text{O}_4\text{Cl}_2$ at ~ 936.5 eV is dominated by contributions from Cu_A $3d_{3z^2-r^2}$ orbitals hybridized with Cu_A $4s$ orbitals, while the peak at 940.7 eV is from $3d_{3z^2-r^2}$ orbitals from either Cu_A and Cu_B which are hybridized with Cu_A $4s$ and Cu_B $4s$ orbitals, respectively. The ratios of the calculated total Cu $3d_{3z^2-r^2}$ to the calculated total Cu $3d_{x^2-y^2}$ hole occupation numbers (0.10 and 0.44 for $\text{Sr}_2\text{CuO}_2\text{Cl}_2$ and $\text{Ba}_2\text{Cu}_3\text{O}_4\text{Cl}_2$, respectively) confirm the experimental results qualitatively and in the case of $\text{Ba}_2\text{Cu}_3\text{O}_4\text{Cl}_2$ even quantitatively. A possible cause for the difference in the Cu $3d_{3z^2-r^2}$ /Cu $3d_{x^2-y^2}$ anisotropy between the two compounds could be again the more closed structure of a Cu_3O_4 plane with respect to a CuO_2 plane.

IV. SUMMARY

To summarize the results, direct experimental information about the unoccupied electronic structure of isolated undoped Cu-O planes in the environment of layered cuprates has been presented. The unoccupied electronic structures of $\text{Sr}_2\text{CuO}_2\text{Cl}_2$ and $\text{Ba}_2\text{Cu}_3\text{O}_4\text{Cl}_2$ are very similar. The UHB's are dominated by contributions from O $2p_{x,y}$ and Cu $3d_{x^2-y^2}$ orbitals thus being electronically two-dimensional as is the case for the UHB's of the high-temperature superconductors. The most important finding of this work is that hybridization with Cu $3d_{x^2-y^2}$ orbitals is not the only mechanism by which the O $2p$ orbitals of these oxychlorides become partly unoccupied. Comparison to calculated partial DOS data reveals that intra- and interplane hybridization with Cu $4p_z$ and Sr $4d$ /Ba $5d$ orbitals is also important. These results are directly relevant to the high-temperature superconductors because of the close similarity of the copper oxychlorides to their undoped parent compounds. Therefore the absorption fine structure encountered in the high-temperature superconductors in the O $1s$ x-ray absorption spectra above the UHB (Ref. 1) is not solely due to oxygen atoms located outside the CuO_2 planes (e.g., in the block layers) but is also derived from oxygen atoms in the Cu-O

planes. In the Cu $2p_{3/2}$ XAS spectra there are transitions into Cu $3d_{3z^2-r^2}$ orbitals at energies above the UHB, which have also been detected in the Cu $2p_{3/2}$ x-ray absorption spectra of the high-temperature superconductors. From a comparison to calculated partial DOS data we conclude that this is due to hybridization with Cu $4s$ orbitals. Differences between $\text{Sr}_2\text{CuO}_2\text{Cl}_2$ and $\text{Ba}_2\text{Cu}_3\text{O}_4\text{Cl}_2$ are the larger width of the UHB and higher relative Cu $3d_{3z^2-r^2}$ hole occupation above the UHB (with respect to the Cu $3d_{x^2-y^2}$ hole occupation in the UHB) in the latter compound. These differences can be thought of being a consequence of the extra Cu_B atoms in the Cu_3O_4 planes of $\text{Ba}_2\text{Cu}_3\text{O}_4\text{Cl}_2$.

ACKNOWLEDGMENTS

Part of this work was funded by the German *Bundesministerium für Bildung, Wissenschaft, Forschung und Technologie* (BMBF) under Contract No. 13N6599/9 and by the European Union (EU) under Contract No. ERB-CHRXCT940438. S. H. acknowledges the *Graduiertenkolleg "Struktur und Korrelationseffekte in Festkörpern" der TU Dresden* (DFG), M. S. G is grateful to the HCM program of the EU for funding. Research at the FU Berlin was funded by the BMBF, Contract No. 13N6601/0 and 05-650-KEA, and the *Deutsche Forschungsgemeinschaft*, Contract No. KA564/7-1. We are grateful to S. -L. Drechsler for helpful discussions.

- ¹J. Fink, N. Nücker, E. Pellegrin, H. Romberg, M. Alexander, and M. Knupfer, *J. Electron Spectrosc. Relat. Phenom.* **66**, 395 (1994).
- ²L. L. Miller, X. L. Wang, S. X. Wang, C. Stassis, D. C. Johnston, J. Faber, Jr., and C.-K. Loong, *Phys. Rev. B* **41**, 1921 (1990).
- ³D. Vaknin, S. K. Sinha, C. Stassis, L. L. Miller, and D. C. Johnston, *Phys. Rev. B* **41**, 1926 (1990).
- ⁴C. Almasan and M.B. Maple, in *Chemistry of High-Temperature Superconductors*, edited by C. N. R. Rao (World Scientific, Singapore, 1991).
- ⁵M. Greven, R. J. Birgeneau, Y. Endoh, M. A. Kastner, B. Keimer, M. Matsuda, G. Shirane, and T. R. Thurston, *Phys. Rev. Lett.* **72**, 1096 (1994).
- ⁶There is superconductivity in $\text{Sr}_2\text{CuO}_2\text{F}_{2+\delta}$ [$T_C = 46$ K, M. Al-Mamouri, P. P. Edwards, C. Greaves, and M. Slaski, *Nature (London)* **369**, 382 (1994)] and $(\text{Ca},\text{Na})_2\text{CuO}_2\text{Cl}_2$ [$T_C = 26$ K, Z. Hiroi, N. Kobayashi, and M. Takano, *ibid.* **371**, 139 (1994)], which are closely related to $\text{Sr}_2\text{CuO}_2\text{Cl}_2$.
- ⁷F. C. Zhang and T. M. Rice, *Phys. Rev. B* **37**, 3759 (1988).
- ⁸M. S. Golden, H. C. Schmelz, M. Knupfer, S. Haffner, G. Krabbes, J. Fink, V. Y. Yushankhai, H. Rosner, R. Hayn, A. Müller, and G. Reichardt, *Phys. Rev. Lett.* **78**, 4107 (1997).
- ⁹B. O. Wells, Z.-X. Shen, A. Matsuura, D. M. King, M. A. Kastner, M. Greven, and R. J. Birgeneau, *Phys. Rev. Lett.* **74**, 964 (1995).
- ¹⁰R. Kipka and H. K. Müller-Buschbaum, *Z. Anorg. Allg. Chem.* **419**, 58 (1976).
- ¹¹S. Noro, H. Suzuki, and T. Yamadaya, *Solid State Commun.* **76**, 711 (1990); S. Noro, T. Kouchi, H. Harada, T. Yamadaya, M. Tadokoro, and H. Suzuki, *Mater. Sci. Eng. B* **25**, 167 (1994).
- ¹²K. Yamada, N. Suzuki, and J. Akimitsu, *Physica B* **213&214**, 191 (1995).
- ¹³F. C. Chou, A. Aharony, R. J. Birgeneau, O. Entin-Wohlman, M. Greven, A. B. Harris, M. A. Kastner, Y. J. Kim, D. S. Kleinberg, Y. S. Lee, and Q. Zhu, *Phys. Rev. Lett.* **78**, 535 (1997).
- ¹⁴H. Rosner, R. Hayn, and J. Schulenberg (unpublished).
- ¹⁵Y. Tokura, S. Koshihara, T. Arima, H. Takagi, S. Ishibashi, T. Ido, and S. Uchida, *Phys. Rev. B* **41**, 11 657 (1990).
- ¹⁶M. Domke, T. Mandel, A. Puschmann, C. Xue, D. A. Shirley, G. Kaindl, H. Petersen, and P. Kuske, *Rev. Sci. Instrum.* **63**, 80 (1992).
- ¹⁷J. J. Yeh and I. Lindau, *At. Data Nucl. Data Tables* **32**, 1 (1985).
- ¹⁸J. Jaklevic, J. A. Kirby, M. P. Klein, and A. S. Robertson, *Solid State Commun.* **23**, 679 (1977); L. Tröger, D. Arvanitis, K. Baberschke, H. Michaelis, U. Grimm, and E. Zschech, *Phys. Rev. B* **46**, 3283 (1992).
- ¹⁹L. H. Tjeng, C. T. Chen, and S. W. Cheong, *Phys. Rev. B* **45**, 8205 (1992).
- ²⁰H. Eschrig, *Optimized LCAO Method* (Springer-Verlag, Berlin, 1989).
- ²¹Transitions into unoccupied Cu $4s$ orbitals are also allowed, but the probability is smaller by a factor of 20 [see, for example, B. K. Teo and P. A. Lee, *J. Am. Chem. Soc.* **101**, 2815 (1979)]. The Cu $2p_{3/2}$ x-ray absorption spectra are therefore dominated by contributions due to transitions into unoccupied Cu $3d$ orbitals, the unoccupied Cu $4s$ orbitals being not visible in the spectra but influencing them via their hybridization with the Cu $3d_{3z^2-r^2}$ orbitals as discussed later in this section.
- ²²This is not the case for $\text{Ba}_2\text{Cu}_3\text{O}_4\text{Cl}_2$ because of the extra hybridization with the Cu_B $3d_{x^2-y^2}$ orbitals.
- ²³The hole occupation number above the UHB is the total hole occupation number minus the hole occupation number in the UHB given in Table I.
- ²⁴The integration was carried out in the same energy range as for the calculated partial DOS.
- ²⁵Matrix element effects have been taken into account.